The Storm Cell Identification and Tracking Algorithm: An Enhanced WSR-88D Algorithm

J. T. JOHNSON,* PAMELA L. MACKEEN,*+ ARTHUR WITT,* E. DEWAYNE MITCHELL,*+ GREGORY J. STUMPF,*+ MICHAEL D. EILTS,* AND KEVIN W. THOMAS*+

* *NOAA, Environmental Research Laboratories, National Severe Storms Laboratory, Norman, Oklahoma*
+ *Cooperative Institute for Mesoscale Meteorological Studies, University of Oklahoma, Norman, Oklahoma*

(Manuscript received 28 February 1997, in final form 9 December 1997)

ABSTRACT

Accurate storm identification and tracking are basic and essential parts of radar and severe weather warning operations in today's operational meteorological community. Improvements over the original WSR-88D storm series algorithm have been made with the Storm Cell Identification and Tracking algorithm (SCIT). This paper discusses the SCIT algorithm, a centroid tracking algorithm with improved methods of identifying storms (both isolated and clustered or line storms). In an analysis of 6561 storm cells, the SCIT algorithm correctly identified 68% of all cells with maximum reflectivities over 40 dBZ and 96% of all cells with maximum reflectivities of 50 dBZ or greater. The WSR-88D storm series algorithm performed at 24% and 41%, respectively, for the same dataset. With better identification performance, the potential exists for better and more accurate tracking information. The SCIT algorithm tracked greater than 90% of all storm cells correctly.

The algorithm techniques and results of a detailed performance evaluation are presented. This algorithm was included in the WSR-88D Build 9.0 of the Radar Products Generator software during late 1996 and early 1997. It is hoped that this paper will give new users of the algorithm sufficient background information to use the algorithm with confidence.

1. Introduction

The network of Doppler radars called Weather Surveillance Radar-1988 Doppler (WSR-88D) have been purchased, installed, and maintained by the United States National Weather Service (NWS), the Federal Aviation Administration (FAA), and the Department of Defense. This modernized network has replaced the aging WSR-57 and WSR-74 radars and become the primary severe weather warning tool used by the government and the private sector. Some advantages of this network are nationwide coverage, Doppler capabilities, and a suite of severe weather detection algorithms. A more complete description of the WSR-88D system is given in Crum and Alberty (1993).

Severe weather detection algorithms are a key element of the WSR-88D system for numerous reasons. Such algorithms can provide severe weather potential and detection products to a forecaster during severe weather warning operations. The WSR-88D algorithms used in NWS offices across the country can detect mesocyclone and tornadic vortex signatures in the Doppler velocity data and furnish continuous isolated storm and storm system identification, tracking, and cell motion products. Many other useful severe weather-related products are discussed in Klazura and Imy (1993).

The subject of this paper is the Storm Cell Identification and Tracking (SCIT) algorithm; many similar algorithms have been developed over the past 40 years. These algorithms have either used cross correlation to determine the movement of storms or storm-cell centroid techniques to individually identify and track storms. Both techniques have strengths and weaknesses: correlation tracking algorithms tend to provide more accurate speed and direction information on larger areas of reflectivity, while centroid identification and tracking algorithms can track individual isolated storms more effectively (Jackson 1993) and can provide cell characteristic information. In addition to these two schemes, a tracking method called combinational optimization, which combines both techniques, has been more recently developed (Dixon and Wiener 1993).

Cross correlation analysis of the reflectivity field was one of the first tracking techniques developed. This method may be used to track the entire reflectivity field (to determine the general motion of the entire field), isolated echo regions (to determine the motion of isolated storms or storm systems), or cells within a large echo region (to determine the motion of cells within a storm system) (Crane 1979). Examples of operational cross correlation algorithms include the Integrated Ter-

Corresponding author address: J. T. Johnson, NOAA/ERL/NSSL, 1313 Halley Circle, Norman, OK 73069.
E-mail: johnson@nssl.noaa.gov

minal Weather System storm cell information algorithm (Klingle-Wilson et al. 1993) and the Advanced Traffic Management System cross-correlation tracker algorithm (Jackson and Jesuroga 1995). Both of these algorithms were initially developed to provide automated storm tracking for the FAA.

The cross-correlation techniques were followed by storm cell centroid identification and tracking techniques. Wilk and Gray (1970) applied a centroid identification technique to the WSR-57 radar signal in order to estimate storm motion and precipitation. Their 2D storm centroid technique identified areas of contiguous echo above a set reflectivity level threshold. An intensity-weighted centroid, used to define the storm location, was determined for each identified area. This technique and variations thereof were also applied by Zittel (1976), Brady et al. (1978), and others. Crane (1979) further developed this type of scheme to define the individual 3D cell cores within clustered or large reflectivity echoes. A few years later, Rosenfeld (1987) developed an algorithm that tracked the cell reflectivity maxima and its encompassing echo. Both algorithms determined the cell volume characteristics associated with identified storm cells. Brady, Crane, and Rosenfeld automated their cell identification and tracking schemes by implementing cell centroid tracking. Boak et al. (1977) developed a centroid identification algorithm and Forsyth (1979) developed a centroid tracking technique. These latter two algorithms became the basis for the WSR-88D storm series algorithm (prior to Build 9.0).

This paper discusses SCIT, an algorithm that was developed to identify, characterize, track, and forecast the short-term movement of storm cells identified in three dimensions. It is based on centroid identification and tracking techniques because of the technique's capability to track individual storms and to provide cell characteristic information. The SCIT algorithm's development was motivated by the relatively poor performance (NSSL 1995) of the WSR-88D storm series algorithms in situations of closely spaced storms (lines, clusters). The use of seven reflectivity thresholds (30, 35, 40, 45, 50, 55, 60 dB*Z*) in the SCIT algorithm, as opposed to the one reflectivity threshold (30 dB*Z*) used in the WSR-88D storm series algorithms, greatly improves identification performance. For instance, within a line or cluster of storms, individual storm cells are detected by the SCIT algorithm, whereas only one storm may be detected by the WSR-88D storm series algorithms. Since SCIT identifies individual storms, rather than storm systems, individual storm cells may be tracked, and their characteristics, such as maximum reflectivity, may be determined and trended. Thus, the evolution of cell-based characteristics is available to the forecaster. This paper describes the details of this algorithm, which has been implemented as part of the WSR-88D system (Build 9.0), including its strengths, weaknesses, and operational performance.

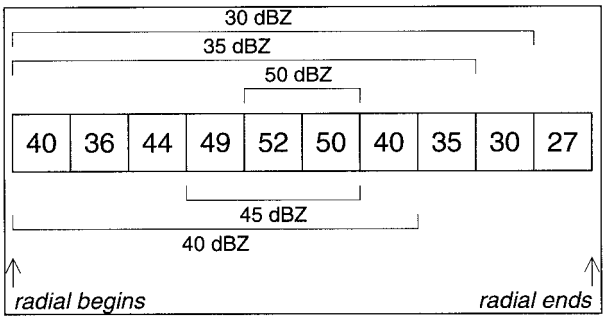

FIG. 1. Identification of 50, 45, 40, 35, and 30 dB*Z* thresholded storm segments along a radial.

2. The SCIT algorithm

a. Data processing requirements

The SCIT algorithm processes volumetric reflectivity information from WSR-88D base data (Crum and Alberty 1993) on a radial-by-radial basis. No velocity data are processed by the algorithm. No special data filtering or thresholding, apart from the radar data acquisition ground clutter suppression, error detection, etc., is performed before data processing begins.

b. Detection methodology

Three-dimensional storm identification is performed in stages, beginning with one-dimensional (1D) data processing. The purpose of the 1D portion of the algorithm is to identify storm ''segments'' in the radial reflectivity data. Storm segments are defined as runs, along a radial, of contiguous range gates (sample volumes) whose reflectivities are above a specified threshold (REFLECTIVITY 1–7; a list of thresholds used by the algorithm is given in appendix A). As illustrated in Fig. 1, when a reflectivity value above REFLECTIVITY is first encountered along a radial, subsequent gates having reflectivity above REFLECTIVITY are grouped together, until a reflectivity value below REFLECTIVITY is encountered. If this reflectivity value is not more than DROPOUT REF DIFF below REFLECTIVITY, DROPOUT COUNT is incremented, and the process continues. However, when a reflectivity value more than DROPOUT REF DIFF is encountered or when the dropout counter (DROPOUT COUNT) reaches a specified value (default = 2), the process is terminated and a storm segment is created. In Fig. 2, three gray-scaled storm segments are shown. Their braced dropout and termination values further illustrate that only dropouts within the segment are saved. The dropout method has been implemented in an attempt to keep related features together.

A storm segment is saved if its radial length (ending range–beginning range) is greater than a preset threshold (SEGMENT LENGTH 1–7; default = 1.9 km). The primary difference between SCIT and the WSR-88D

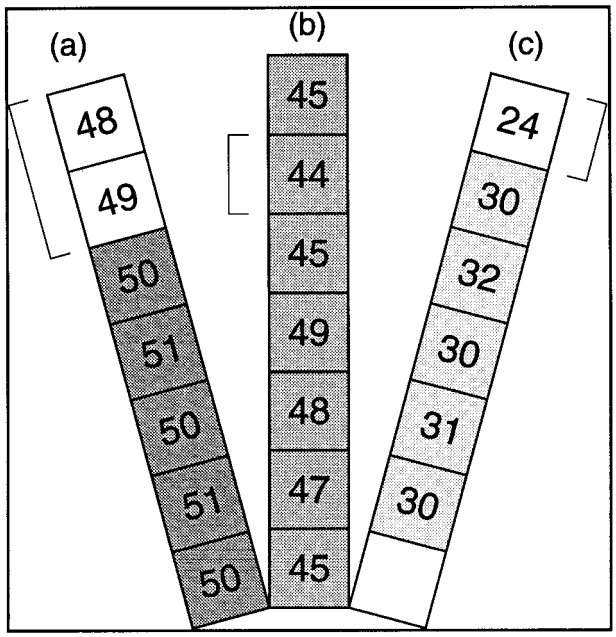

FIG. 2. The shaded areas represent the saved portions of the following storm segments (braces indicate dropouts or termination values): (a) 50-dBZ storm segment followed by two dropouts, (b) 45-dBZ storm segment with one dropout, and (c) 30-dBZ storm segment followed by a reflectivity value less than the dropout value (termination value).

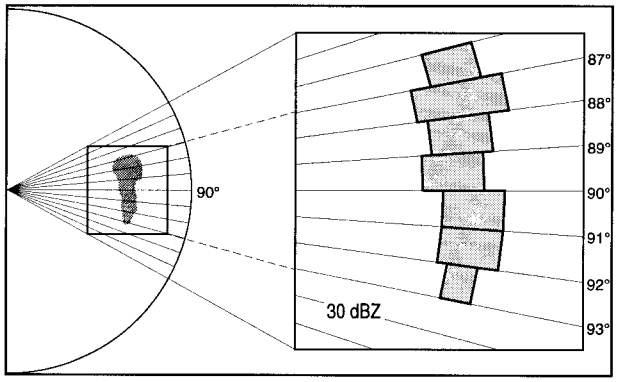

FIG. 3. Outlined blocks represent 30-dBZ thresholded storm segments. All the 30-dBZ storm segments are combined into a 2D component, assuming that they meet the azimuthal and range criteria.

storm segments algorithm for this process is that SCIT repeats the process using seven different reflectivity thresholds (REFLECTIVITY: 60, 55, 50, 45, 40, 35, and 30 dBZ), whereas the WSR-88D storm segments algorithm uses only one threshold (30 dBZ).

After the last radial of an elevation scan has been analyzed, individual storm segments are combined into 2D storm components based on spatial proximity. To qualify for combination, storm segments must be close to one another azimuthally (within AZIMUTHAL SEPARATION; default = 1.5°) and overlap in range by a threshold value (SEGMENT OVERLAP; default = 2 km). Figure 3 shows a 30-dBZ 2D storm component containing seven storm segments. Storm components must have at least two storm segments (NUMBER OF SEGMENTS; default = 2) and an area larger than COMPONENT AREA (default = 10 km^2). Feature core extraction is employed to isolate the cells from surrounding areas of lower reflectivity. If the centroid of a higher-reflectivity thresholded component falls within the area of a lower-reflectivity thresholded component, the latter component is discarded (see Fig. 4).

Following the processing of all elevation scans within the current volume scan, the components are sorted by decreasing mass, and vertical association is attempted. The component mass is an estimate (based on its reflectivity) of the component's equivalent liquid water content. Each identified 3D storm cell consists of two or more 2D storm components on consecutive elevation angles. The process of vertical association is an iterative one, beginning at the lowest elevation angle. First, an attempt is made to associate components (on consecutive elevation scans) whose centroids are horizontally within 5 km of one another. If more than one association is possible, association is made with the 2D component having the largest mass. When nonassociated components remain after the first attempt, the search radius is increased to 7.5 km, and the process is repeated for all the nonassociated components. If, after this second attempt, nonassociated components still remain, a final attempt is made using a 10-km search radius. All remaining nonassociated components are saved but are not currently used in the algorithm as implemented in the WSR-88D system. The process is performed for all adjacent elevation scans. An example of an ideal 3D storm cell identification is shown in Fig. 5. The final result is a group of 3D and 2D storm cell snapshots. Since only the most intense (highest-reflectivity thresholded) components are used to define 3D storm cells,

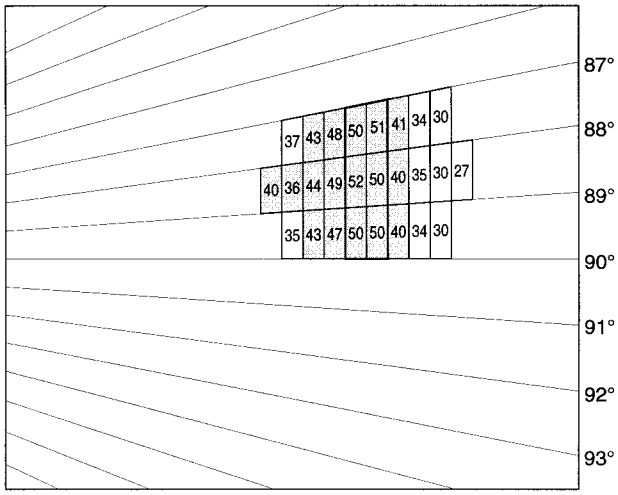

FIG. 4. Two 2D components (40 and 50 dBZ) within a cell feature. A 45-dBZ 2D component is also embedded within the shaded area.

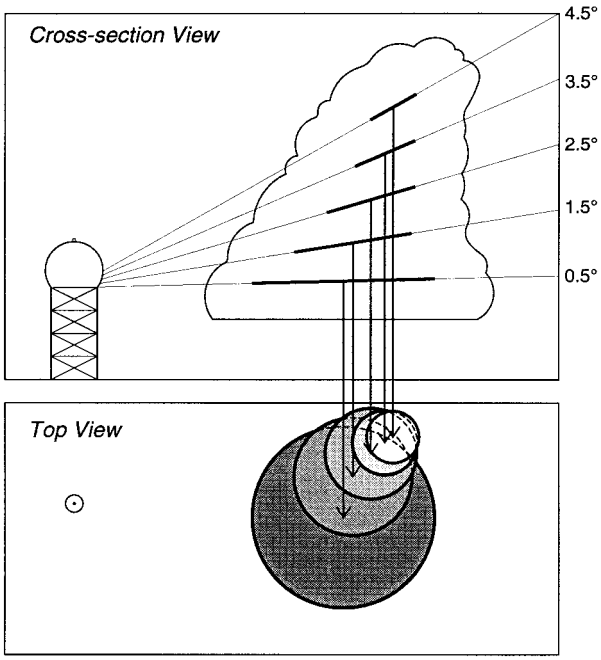

FIG. 5. The highlighted segments and their corresponding circles represent 2D components.

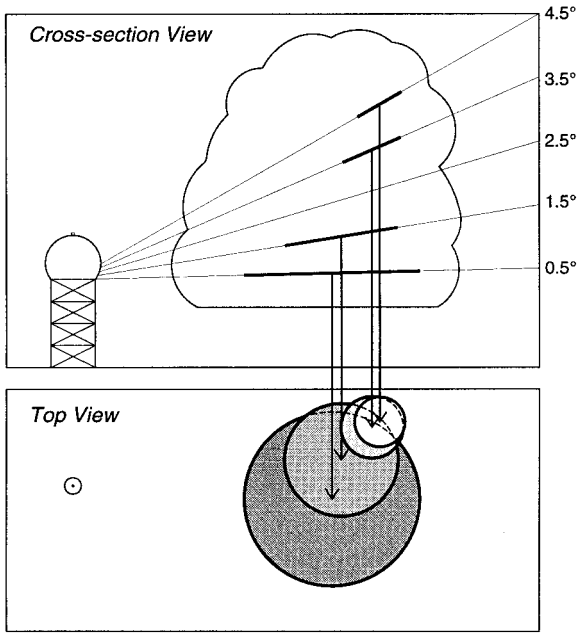

FIG. 6. Similar to Fig. 5 except with a vertical gap in the detected 2D components.

the final product is actually a 3D storm cell centroid. These storm cells are then ranked by their cell-based vertically integrated liquid (VIL) value (see appendix B).

The SCIT implementation in the WSR-88D system does not utilize the 2D centroid information from the nonassociated components. After all possible 3D associations are completed, the remaining nonassociated lowest-elevation 2D centroids located beyond a site-adaptable range threshold could be classified as 2D storm cells. This new classification would identify storm cells as undersampled by the radar due to their range from the radar. A similar procedure is implemented in the National Severe Storms Laboratory (NSSL) Mesocyclone Detection Algorithm (Stumpf et al. 1998).

Occasionally, when several cells are clustered closely together, the algorithm may have difficulty identifying distinct 2D components for each cell at all of the elevation angles. When this happens, a single storm cell may actually be detected as two (or more) 3D cells, each at roughly the same horizontal location but separated by a vertical gap. As shown in Fig. 6, under certain circumstances, the collocated 3D cells may be combined to form a single cell. This is done when the following three conditions are met: 1) the two cells do not have 2D storm components at the same elevation angle (i.e., there is a vertical gap), 2) the horizontal distance between the two centroids is less than a preset threshold (HORIZONTAL MERGE; default = 10.0 km) and 3) if the vertical separation between the top of one cell and the base of the other is less than both of the following parameters: HEIGHT MERGE; default = 4.0 km, and ELEVATION MERGE; default = 3.0°.

Since the new algorithm detects many more storm cells than the WSR-88D storm series algorithms, there can be situations where numerous cells are identified in close proximity to one another. This may result in undesirable crowding of displayed output and poor tracking performance. In such situations, it is preferable to retain only the stronger, taller storm cells. Thus, if the distance between the centroids of two cells is less than a preset threshold (HORIZONTAL DELETE; default = 5.0 km), the weaker or shorter cell is discarded if a difference in depth greater than DEPTH DELETE (default = 4 km) exists between the two cells.

c. Tracking methodology

Storm cells identified in two consecutive volume scans are associated temporally to determine the cell track. The initial step is to check the time difference between volume scans. If this time difference is greater than TIME (default = 20 min), time association is not attempted. This is done to handle data discontinuities due to malfunctions in the radar or interrupted communications.

Using the centroid locations from the previous volume scan, a first guess at location for the current volume scan is generated. The first guess uses either the cell's previous motion vector or a default motion vector (if the cell was first detected in the previous volume scan). The default motion vector is either an average of all the motion vectors from storm cells in the previous volume scan or from user input (SPEED, DIRECTION). The

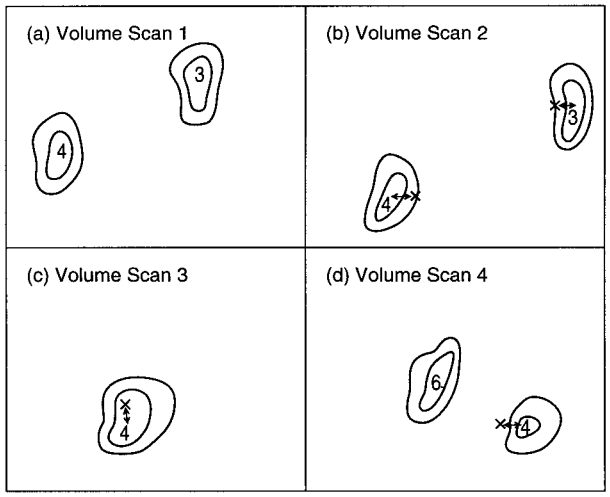

FIG. 7. An example of the time association process. The × represents the current volume scan cells' first-guess position and the short arrows show the forecast error between the previous volume scan cells' position and their associated first-guess positions.

latter is used only if no average motion vector could be determined from the previous volume scan. Future enhancements to the algorithm should include accepting input from a sounding in the form of the mean 0–6-km wind vector (Davies and Johns 1993) or some other mean wind.

Next, the distance between the centroid of each cell detected in the current volume scan and each of the first-guess locations is calculated. If the distance is less than a threshold value, the old cell associated with that first-guess position is saved as a possible match with the current cell. Then, the distance between the new cell and all possible matches is determined. The match with the smallest distance is considered to be the time association of the detected cell. The last step involves calculating a new motion vector for each storm cell that has been identified for at least two volume scans. The motion vector is computed using a linear least squares fit of the storm cell's current and up to 10 previous locations. Equal weight is given to all previous positions.

An example of the time association process is shown in Fig. 7. The initial detection of two storm cells is depicted in Fig. 7a. Figure 7b illustrates the second detection of two storm cells, their first guess positions (denoted by an "×"), and the distance between the old and current storm cell position (denoted by double arrowed line). Assuming that the computed distance meets threshold requirements, both cells are time-associated with their previous detections.

Once the tracking process is completed, attributes of the storm cells are calculated and stored as a time series for up to the previous 10 volume scans. See Table 1 for a list of relevant attributes.

TABLE 1. Parameters for which the SCIT algorithm produces a time series. An asterisk denotes those parameters not available to the end user of the WSR-88D implementation of the SCIT algorithm.

Maximum reflectivity
Height of maximum reflectivity
Base (height of lowest 2D feature)
Top (height of highest 2D feature)
Mass
Cell-based VIL [vs the traditional grid-based VIL (Greene and Clark 1972)]
Height of center of mass
*Volume
*Core aspect ratio (ratio of the depth of the identified storm cell's core to its width)
*Ratio of maximum reflectivity to reflectivity at the lowest elevation angle

3. Performance evaluation

The SCIT algorithm's performance was evaluated for 1) cell identification, 2) cell tracking, and 3) position forecasting. A discussion of the evaluation procedure is presented, followed by the results. The identification results are stratified by storm type and are compared to the performance of the WSR-88D storm series algorithms. The tracking evaluation demonstrates how well the detected storms are correctly associated in time and the forecasting evaluation provides the average error associated with multiple forecast periods.

a. Identification evaluation

The following procedure was followed to determine SCIT algorithm identification performance for each case in the dataset:

1) verification dataset was determined,
2) algorithm was run on each case,
3) the output was scored versus verification, and
4) characteristics of algorithm failures were identified.

To determine the performance of the algorithm for various different environments, cases were subjectively stratified into the following categories:

1) "isolated nonsevere": storms were predominantly isolated and no severe weather reports were recorded,
2) "isolated severe": storms were predominantly isolated and more than one severe weather report was recorded,
3) "MCS (mesoscale convective system)/Line": individual storms were in a large cluster or line,
4) "minisupercell": storms took on the structure of classic supercell storms, but the horizontal and vertical scale was much less than classic (Burgess et al. 1995), and
5) "stratiform precipitation": a large area of light to moderate reflectivity with few if any reflectivity values above 40 dBZ.

These categories were chosen because they represent

TABLE 2. Cases chosen for the SCIT algorithm evaluation and their storm type.

Radar and city	Date	Total # human-verified cells	Storm type
KFDR, Frederick, OK	20 April 1992	368	Isolated severe
KOUN, Norman, OK	2 September 1992	473	Isolated severe
KMLB, Melborne, FL	25 March 1992	734	MCS
KMLB, Melborne, FL	9 June 1992	591	Isolated nonsevere
KMLB, Melborne, FL	12 June 1992	580	Isolated nonsevere
KLSX, St. Louis, MO	8 June 1993	512	MCS/Line
KLSX, St. Louis, MO	2 July 1993	325	Line
KTLX, Oklahoma City, OK	18 June 1992	147	Isolated severe
KTLX, Oklahoma City, OK	21 February 1994	116	Stratiform
KIWA, Phoenix, AZ	6 August 1993	867	Isolated severe
KIWA, Phoenix, AZ	20 August 1993	832	Isolated severe
KLWX, Sterling, VA	14 April 1993	282	Minisupercell
KLWX, Sterling, VA	1 May 1994	218	Minisupercell
KLWX, Sterling, VA	6 October 1995	237	Minisupercell
KCBX, Boise, ID	1 May 1995	129	Isolated severe
KBIS, Bismark, ND	21 May 1995	152	Isolated nonsevere
KBIS, Bismark, ND	7 June 1995	235	MCS/Line
Total		6561	

the scenarios that the algorithm must successfully handle for deployment in the nationwide WSR-88D network. Isolated storms were subdivided into severe and nonsevere because severe storms tend to be much larger and have a multicellular structure. MCSs and lines were combined into one category because they represent the same problem to the algorithm: closely spaced cells that often evolve quickly with motion typically different from that of the entire complex. Minisupercells were made a separate category to demonstrate algorithm performance on ''nonclassic'' type of isolated severe storms. Stratiform cases were used in the evaluation simply to demonstrate the algorithm's limitation for this type of scenario.

Table 2 lists the cases and their classifications. Each case is comprised of about 1 h of data.

The verification set for each case was determined through visual inspection of the radar data. After discussions with many operational and research meteorologists, a set of verification rules was developed. An area of reflectivity was considered a storm cell if:

1) it had a maximum reflectivity of at least 30 dB*Z*,
2) it had a horizontal 30-dB*Z* area of at least 5 km^2 on at least one elevation scan,
3) its estimated 3D mass-weighted centroid was separated from other centroids by at least 5 km, and
4) the area was separated from other areas by a local minimum at least 10 dB*Z* lower than the maximum within the area.

Note that these rules do not include a criterion for depth. Thus, if an area of reflectivity meets all of the above criteria on at least one elevation scan, the area is considered a storm cell for verification purposes. The SCIT algorithm requires that an area of reflectivity meet size and intensity criteria on at least two consecutive elevation scans to be declared a storm cell. This algorithm requirement is to avoid identification of ground clutter as storm cells; however, this can also cause shallow cells to be missed. We will discuss the impact this has on the performance results later.

Using NSSL's Radar Algorithm and Display Software (Sanger et al. 1995), radar meteorologists examined reflectivity data in accordance with the verification rules. Both composite reflectivity data and individual elevation scans were used to verify which areas of reflectivity were cells. The 30-dB*Z* area and the horizontal location of the 3D mass weighted centroid for each verification cell were estimated using the composite reflectivity field. The 30-dB*Z* area was estimated using a circular approximation with the radius of the estimated circle being recorded for verification. The maximum reflectivity value, azimuth, and range were also recorded for each storm cell. These characteristics constitute the verification set for each case. Both the SCIT algorithm and the WSR-88D storm series algorithm were run using the default algorithm settings (see appendix A for SCIT settings). The horizontal location (azimuth and range) of each algorithm-identified storm cell was then compared to the verification dataset.

Figure 8 shows the method to determine hits, false alarms, and misses. If an algorithm detection exists within the radius of a human-verified cell, the detection is declared a ''hit.'' Conversely, if a verified cell does not have an associated algorithm detection, the algorithm is assessed a ''miss.'' If an algorithm detection exists outside of all verified cells' radii, the detection is declared a ''false alarm.''

The algorithm's output as compared to the verification dataset, and the probability of detection and false alarm rate (Wilks 1995) was calculated for each storm type and in total. Table 3 presents the results of the SCIT performance evaluation. The results show that cells above 40 dB*Z* have a 68% chance of being detected and

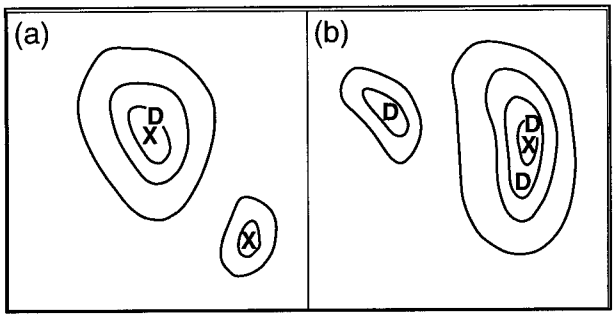

FIG. 8. Algorithm detected cells are denoted by D, whereas verified cells are denoted by X. In (a) a hit and a miss are shown. The hit is the cell with closely coinciding X and D notations. In (b) two false alarms are shown. The false alarms are the cells solely noted by a D not directly adjacent to an X.

that cells with reflectivities above 50 dB*Z* have a 96% chance of being detected. Also, on average, the results for isolated cells are better than for other types. A note concerning the stratiform precipitation event: the algorithm was not designed to perform well on such an event. The inclusion of the results for this event illustrate this fact. The 0% probability of detection (POD) for 30–39-dB*Z* cells is an indication that these cells did not demonstrate much vertical growth and thus the algorithm's requirement for two consecutive elevation scans eliminated the possibility of detecting these cells.

No false alarms occurred in these cases; however, known instances of false alarms involve nonmeteorological radar returns, such as chaff or ground clutter. The algorithm requirement of two consecutive elevation angles eliminates a large majority of these potential false alarms.

Algorithm misses were each analyzed to determine their cause. Two types of algorithm failures were identified: 1) decaying or newly formed cells not being identified when in the vicinity of larger mature cells, and 2) cells meeting size and intensity criteria on only one elevation scan not being identified.

Misses of decaying or newly formed cells were due to one of the algorithm's cell definition rules. When the centroid of a 2D reflectivity component exists within the horizontal radius of another component (at the same elevation), the component with the higher reflectivity is saved and the other is discarded. In each case, the cell affected by this rule was either in its decaying or formative stage. For example, in Fig. 9, a storm cell to the northeast of storm cell 21 is in its decaying stage; a component is defined on the lowest-elevation scan (left panel). However, at the next higher-elevation scan (right panel), only the cell to its south has a definable component whose threshold is greater than the larger, weaker components enclosing both cells. As a result, the decaying cell is not detected.

Algorithm misses due to lack of vertical continuity were ''too shallow'' to pass the size and intensity thresholds on two consecutive elevation scans. An example of this type of miss is shown in Fig. 10. These misses caused by shallow cells were further analyzed to determine their characteristics. These missed cells were all small in size (2D areas <10 km^2) and weak in reflectivity (maximum reflectivity <45 dB*Z*). There is also some indication that storms located more than 150 km from the radar site are more likely to be missed, which is likely related to a radar's poor vertical resolution at long ranges due to beam spreading. A range-adaptable, 2D cell detector has been developed to detect such cells. However, this technique was not implemented in the WSR-88D in Build 9.0.

TABLE 3. Probability of detection (POD) for each storm type in the identification performance evaluation for the SCIT algorithm.

Storm type	POD (cells 30–39 dBZ)	POD (cells 40–49 dBZ)	POD (cells $\geq$ 50 dBZ)
Isolated severe	27%	70%	96%
Isolated nonsevere	43%	68%	97%
MCS/Line	25%	64%	96%
Stratiform	0%	13%	—
Minisupercell	71%	82%	96%
Total	28%	68%	96%

The WSR-88D storm series algorithms were also run on each of the cases listed in Table 2. Using the same verification dataset and the same scoring techniques as for the SCIT algorithm, the WSR-88D algorithm output was scored versus the verification data for each case. The performance results for each type are given in Table 4. Like the SCIT algorithm, the WSR-88D storm series algorithms tend to better identify isolated storm cells than closely spaced cells that exist within multicellular thunderstorms and squall lines. However, these results also show that using only one reflectivity, rather than seven reflectivity thresholds (see Table 3), as a discriminator for cell detections results in much poorer storm cell detection, regardless of storm type or storm cell intensity. As with SCIT, there were no false alarms.

b. Tracking performance evaluation

Correct time associations are essential for an end user to follow cell evolution. A correct time association refers to a case in which a cell was correctly identified and correctly tracked. In these cases, the calculated cell evolution characteristics may be used with some confidence. The tracking performance evaluation involves four steps:

1) tracking the volume scan-to-volume scan life cycle of all algorithm-identified cells,
2) determining the number of incorrect time associations,
3) noting their characteristics, and
4) calculating the percentage of cells correctly tracked by the algorithm.

The ''percentage correct'' is simply the ratio of the cor-

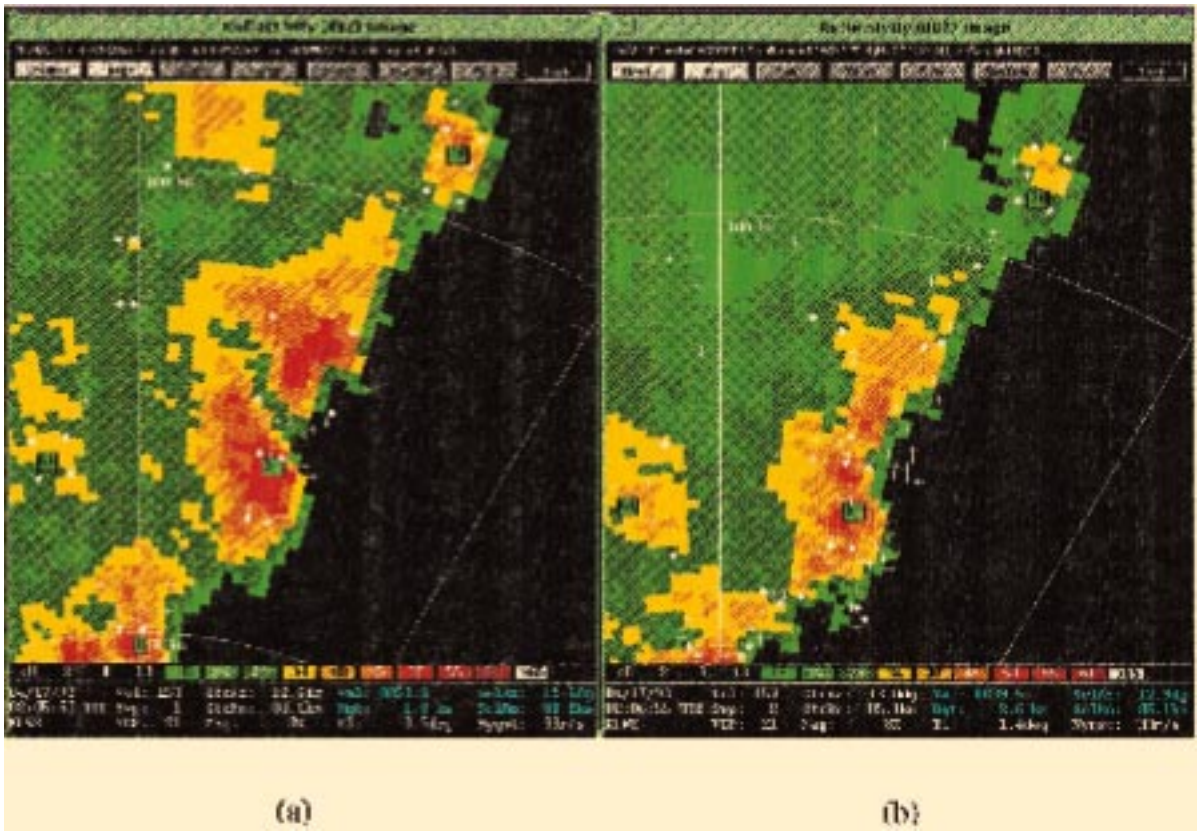

FIG. 9. Example of a storm not meeting all criteria on at least two consecutive elevation angles: (a) a component is defined on the lowest elevation scan (defined by the four white dots); (b) on the second elevation scan, only the cell to its south has a definable component whose threshold is greater than the larger, weaker components enclosing both cells.

rect time associations divided by the total number of time associations. Four cases were evaluated: two mini-supercell cases, one isolated severe case, and one MCS/Line case. The results are given in Table 5.

Most time association errors occur during the simultaneous growth and decay stages of two different closely spaced cells (see Fig. 11). In the first composite reflectivity image a new cell appears to be forming within cell 17's forecast path. Indeed, in the second image, SCIT detects the new cell but incorrectly time-associates it with dissipating cell 17. As a result, the new cell's observed characteristics are incorrectly time-associated with the dissipating cell's and vice versa. In this example, the new storm formed very near the forecasted cell position. Sometimes new storm cells are within the thresholded distance requirement, but their position is so angularly offset from the forecast position that a time association between the two cells is clearly incorrect. This type of error may be eliminated by imposing a directional thresholding rule to the time association process. For instance, a 90° threshold would limit cell time association to within 45° of either side of a forecasted position. Figure 12 shows an example of the implementation of this technique. However, such a technique has problems with slow-moving storms that may make apparently large changes in direction, so at this time, this technique has not been implemented.

c. Positional forecasting evaluation

An analysis of SCIT forecasting performance was carried out for 898 cells (with a lifetime of at least two volume scans) for a variety of storm types. The analysis involved a comparison of SCIT-identified storm location (at the time of the forecast) to the forecast location and computing the distance between the two. The results for different lead times were averaged to find the mean forecast error. This was done for forecast lead times out to 60 min. The results are given in Table 6. As is expected, forecast error increases with lead time.

4. Products

The WSR-88D Build 9.0 version of the SCIT algorithm creates tabular, alphanumeric, and graphical products. The products provide storm cell attribute information on storm structure along with tracking information that aid the user during the forecast and warning process. Storm track attributes are available in each format whereas storm structure attributes are only given

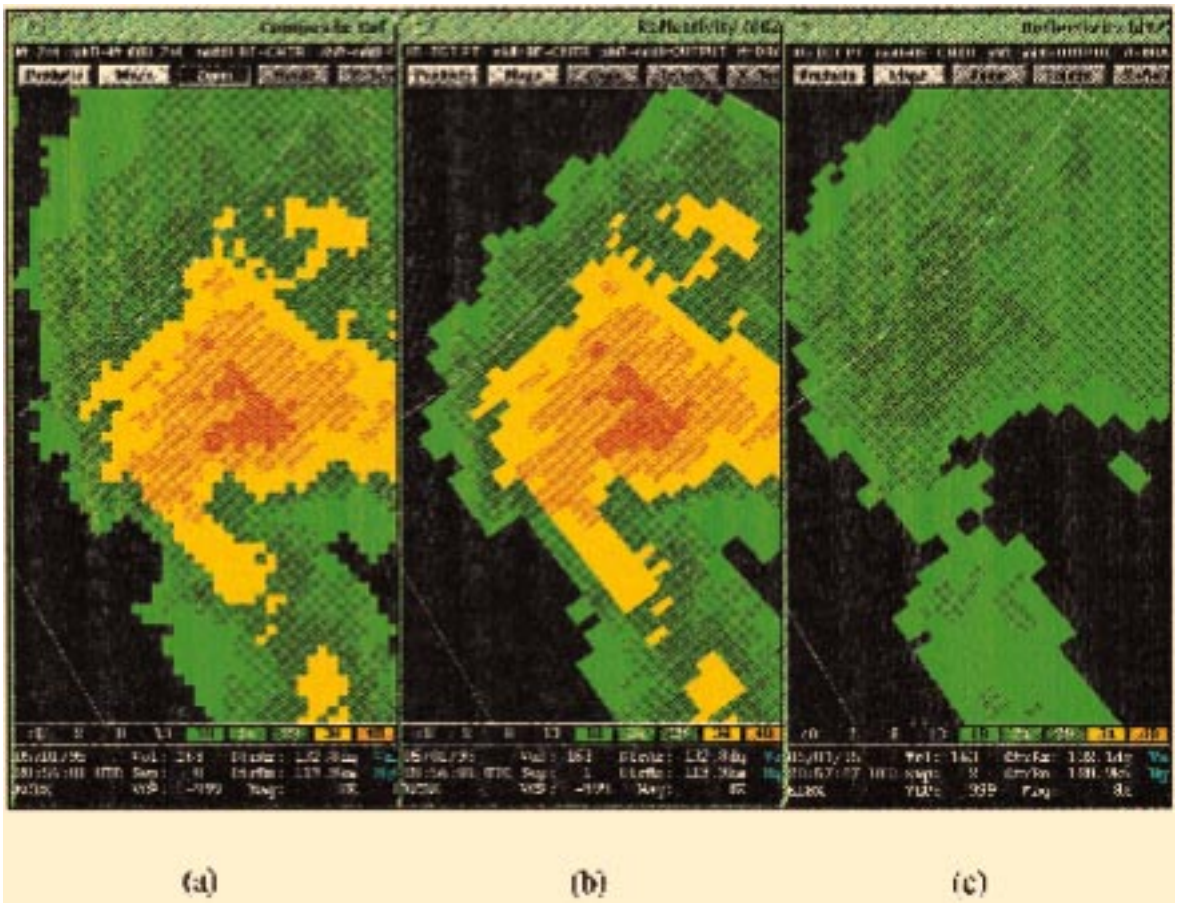

FIG. 10. Example of a ''shallow'' cell lacking vertical continuity (reflectivity field on second elevation scan is less than 30 dBZ). These three consecutive images show the (a) composite reflectivity field, and (b) the first and (c) second elevation scans from Boise, Idaho, on 1 May 1995.

in alphanumeric format. Storm structure trends may be displayed graphically on the Principle User Processor (PUP).

The storm structure and tracking attributes are shown in Table 7. A number of graphical storm track products are also available; a subset is described here. For example, the past positions (up to the number of past volumes) and the 15 min extrapolated positions may be displayed. To reduce crowding, one may limit the displayed number of cells to those with ''high'' cell-based (VIL) values. Further reduction in crowding may be accomplished by turning off the past locations and/or forecast locations. Trends of the attributes (as noted by an asterisk in Table 7) may also be displayed on the PUP.

5. Summary

The SCIT algorithm's development was motivated by the oftentimes poor performance of the WSR-88D storm series algorithms in situations of closely spaced storms (lines, clusters). As the identification statistics show, the use of seven reflectivity thresholds in the SCIT algo-

TABLE 4. Probability of detection (POD) for each of the chosen storm types for the WSR-88D storm series algorithms.

Storm type	POD (cells 30–39 dBZ)	POD (cells 40–49 dBZ)	POD (cells ≥ 50 dBZ)
Isolated severe	14%	21%	61%
Isolated nonsevere	21%	33%	45%
MCS/Line	18%	23%	35%
Stratiform	0%	7%	—
Minisupercell	4%	24%	30%
Total	17%	24%	41%

TABLE 5. The percentage of correct time associations from the SCIT algorithm for each case.

Case	Number of time assoc.	Case type	% Correct time associations
KLWX 041693	236	Minisupercell	96%
KLWX 050194	178	Minisupercell	97%
KCBX 050195	86	Isolated severe	91%
KBIS 060695	253	Multicellular	96%

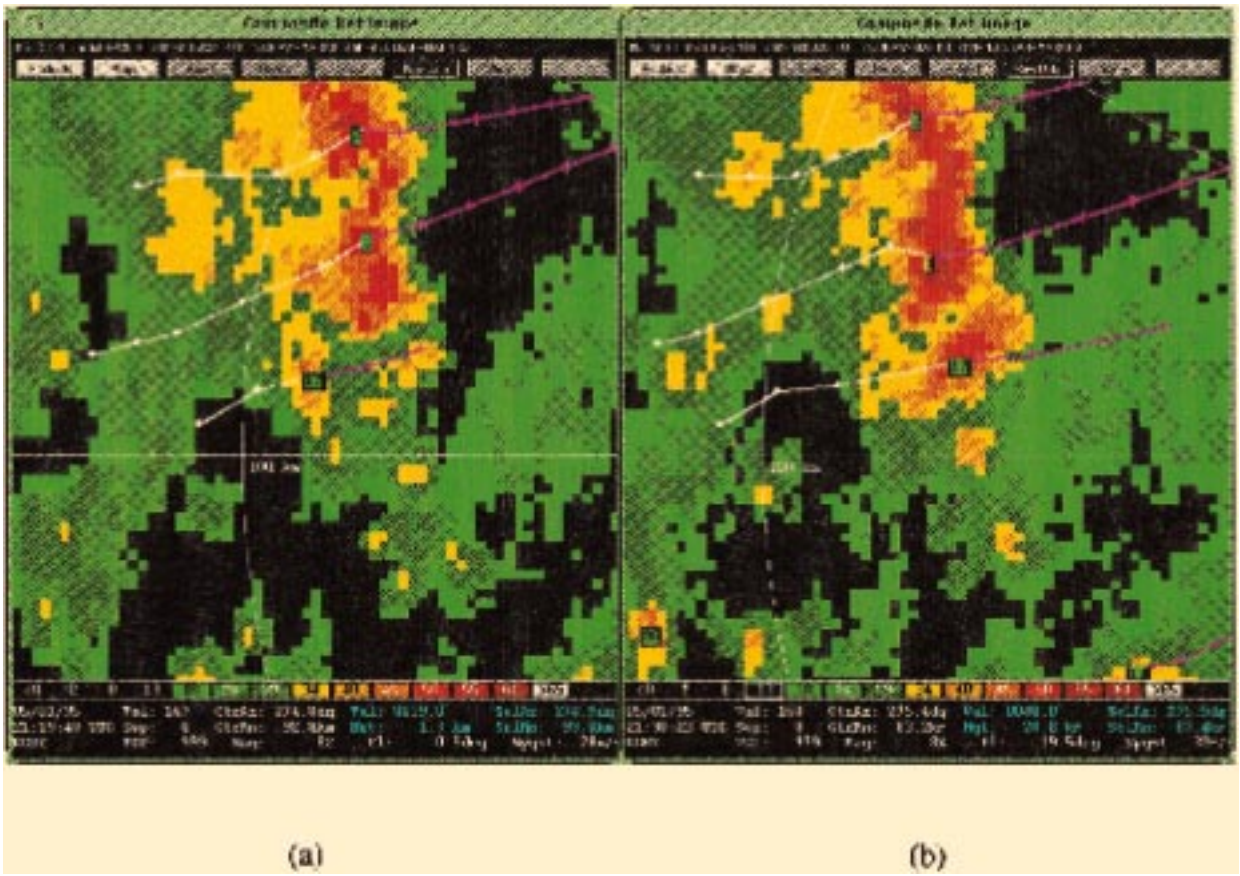

FIG. 11. (a) Composite reflectivity image (volume scan 167) where a new cell appears to be forming within cell 17's forecasted path. (b) Next volume scan (168) SCIT detects the new cell but incorrectly time associates it with dissipating cell 17.

rithm, as opposed to one in the storm series algorithm, greatly improves the identification of storm cells.

The SCIT algorithm uses thresholds of reflectivity, length of segments, and area of components (as well as other thresholds), and it requires at least two consecutive elevation angles of information for ranges less than or equal to a threshold, to detect a storm. Thus, the algorithm does not detect cells that are small (either in length along a radial or in areal coverage), shallow (not passing thresholds on two consecutive elevation scans), or have a maximum reflectivity less than 30 dB*Z* (e.g., developing storms, towering Cu). However, when storm cells form within extremely close proximity to each other, the above thresholds may merge cells together and identify them as one cell. This scenario tends to occur in squall lines with large areas of similar reflectivity.

Since the SCIT algorithm detects more storm cells than the storm series algorithm, the tracking process becomes much more complicated. The simple tracking technique used in the SCIT algorithm performs best when storms have fairly consistent velocities and new storms do not develop close to dissipating storms. Therefore, isolated storms and well-organized storms within squall lines, clusters, etc., that have consistent velocities are tracked with the greatest accuracy. Finally, the forecast performance analysis shows that short-term storm position forecasts tend to be more accurate than longer-term forecasts.

6. Operational implications of the SCIT algorithm

Now that the SCIT algorithm has replaced the WSR-88D storm series algorithm as the fielded storm identification and tracking algorithm for the WSR-88D, several changes in strategy for storm detection and algorithm guidance usage are warranted. Although the SCIT algorithm represents a vast improvement over the storm series algorithm, users should be fully aware of SCIT's strengths and weaknesses.

As the new SCIT algorithm has greater precision in identifying individual storm cells versus larger areas of precipitation, users may still find it important to be able to track larger areas of precipitation. We would not recommend the use of the WSR-88D storm series algorithm, with its single 30-dB*Z* threshold, to track mesoscale stratiform areas of precipitation. Nor do we advocate the use of lowered thresholds (by changing REFLECTIVITY in appendix A) to mimic the former

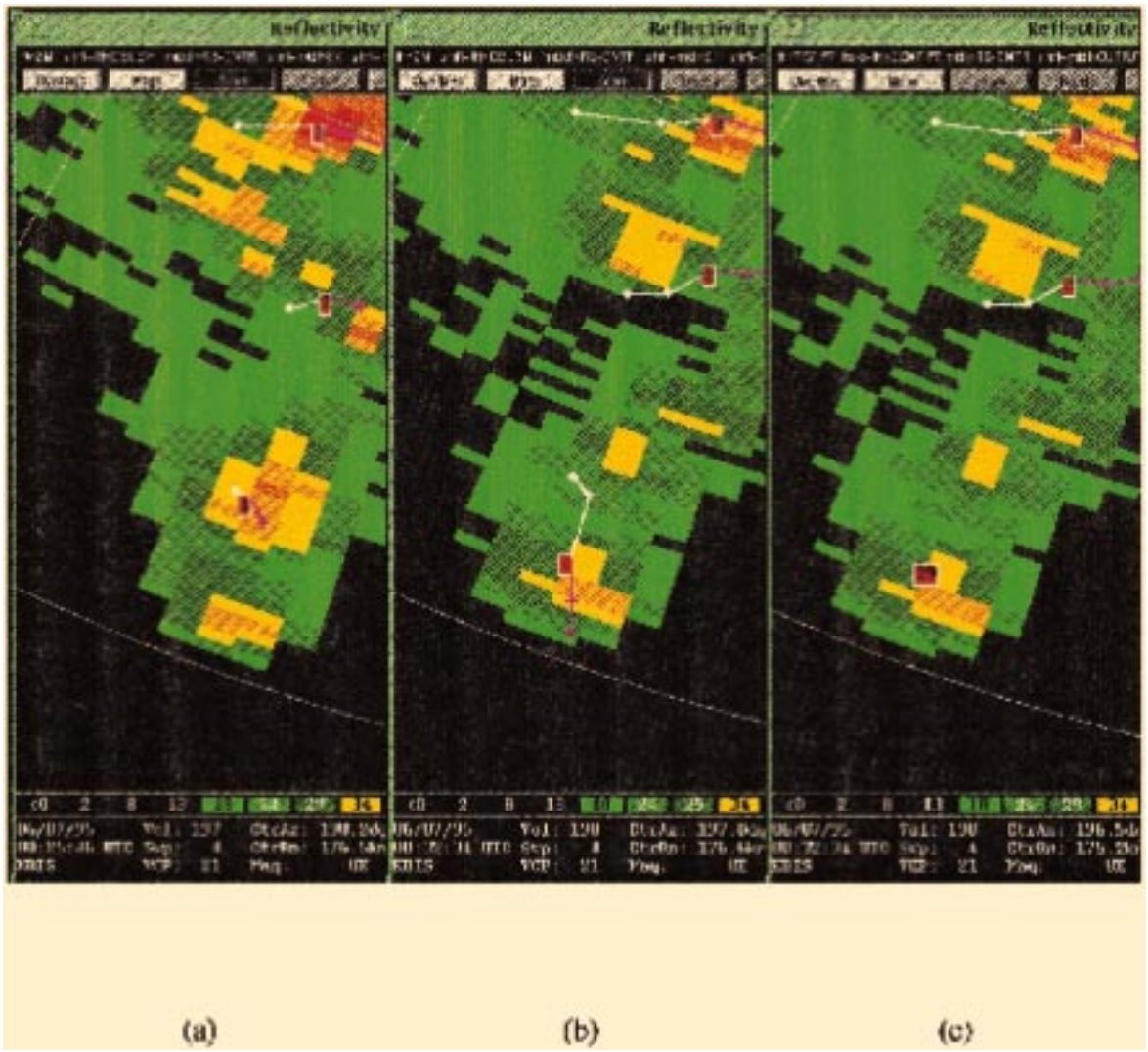

FIG. 12. (a) Volume 197, fourth elevation scan; a new cell is forming to the south of cell 1. (b) Volume 198, fourth elevation scan; the new cell is incorrectly time associated with cell 1, which is dissipating. (c) After implementing a 90° directional threshold, this image shows a correctly, newly identified cell 29.

algorithm. These large areas of precipitation (e.g., trailing stratiform areas of mesoscale convective systems) are not storm cells and cannot be accurately tracked using a centroid-based cell algorithm. An area-based tracking algorithm, such as those developed by Jackson and Jesuroga (1995) and Klingle-Wilson et al. (1993), would be more attuned to tracking these mesoscale features. We suggest that future work should include the development of an area-based tracking element to a precipitation-tracking algorithm to compliment the cell-based tracker of SCIT.

TABLE 6. Average forecast error for given forecast lead times for the SCIT algorithm.

Forecast time (min)	Number of cells in sample	Average forecast error (km)
5	898	2.0
15	498	5.0
30	227	9.9
45	109	15.2
60	55	22.8

TABLE 7. Listing of storm structure and tracking attributes. (An asterisk indicates trend information may be displayed on the PUP.)

Storm structure attributes	Tracking attributes
Storm ID	Storm ID
Storm position	Current storm position
Cell-based VIL	Position movement
*Storm top	Forecast positions
*Storm base	Forecast error
*Maximum storm reflectivity	
*Maximum storm reflectivity altitude	

Furthermore, the rapid evolution of storm cells presents some challenges in separating out individual cell elements from multicell and supercell severe storms. These kinds of storms exhibit series of developing, mature, and decaying cells, sometimes in close proximity to each other, and with some degree of vertical tilt. Their isolation by a cell-based algorithm remains a challenge.

Finally, users should be cognizant that any cell centroid identification and tracking algorithm does exactly what it is designed to do, namely, detect and track the cell *centroid* or center. The center of a storm does not always denote the areas of threatening weather with that cell. It is more appropriate for users to be aware that the onset of a storm (its leading edge) is a better discriminator of the beginning of any severe weather warning. We recommend that a future SCIT algorithm contain cell detection and tracking, area tracking (for squall lines), and a leading-edge detector to facilitate the warning process.

Acknowledgments. Thanks to Mike Francis, Steve McIntosh, and Robert Harron for their contributions toward the performance evaluation, and to Rodger Brown for his guidance through the completion of this project. Additional thanks to Irv Watson for reviewing this manuscript and many insights into the development of the algorithm. Funding for this work was partially provided by the National Weather Service Operational Support Facility and the Federal Aviation Administration.

APPENDIX A

SCIT Algorithm Adaptable Parameter Settings

Below are the parameter settings for the SCIT algorithm as implemented by the Operational Support Facility in the WSR-88D Build 9.0 software. Note that this does not constitute all the adaptable parameters in the algorithm.

1) AZIMUTHAL SEPARATION
   Definition: Maximum azimuthal separation allowed for grouping segments into 2D components.
   Algorithmic response to change: In general, there is little effect in increasing the maximum azimuthal separation except where storms are ''affected'' by blockage. The value of the parameter should never go below the azimuthal separation of the radar data or no storms will be identified.
   Values: Default 1.5°, range (1.5°–3.5°)
2) COMPONENT AREA 1–7
   Definition: Area threshold for features to be considered as storm components for each of the seven reflectivity thresholds (60–30 dB*Z*).
   Algorithmic response to change: Lowering this parameter will cause the detection of smaller storms and raising this parameter will decrease the number of detections.
   Values: Default 10.0 km^2, range (10.0–30.0 km^2)
3) DEPTH DELETE
   Definition: Threshold depth used, when two cells are in close proximity, to determine that the weaker cell should be deleted in order to avoid cell crowding.
   Algorithmic response to change: A larger (smaller) value will result in fewer (more) small, weak storms being detected in close proximity to other stronger storms.
   Values: Default 4.0 km, range (0.0–10.0 km)
4) DIRECTION
   Definition: Default direction assigned to storm cell when DIRECTION is not available.
   Algorithmic response to change: Changing this value will assign a new default storm direction.
   Values: Default 225°, range (0°–360°)
5) DROPOUT COUNT
   Definition: Maximum number of contiguous sample volumes with a reflectivity below the threshold REFLECTIVITY by less than or equal to DROPOUT REF DIFF that may be included in a segment identified with that REFLECTIVITY.
   Algorithmic response to change: Setting this threshold lower will cause more strict adherence to the threshold REFLECTIVITY when building segments (i.e., small changes in reflectivity just below the threshold REFLECTIVITY will not be allowed in the segment). Setting this threshold higher will cause less strict adherence to the threshold REFLECTIVITY when building segments (i.e., larger changes in reflectivity below the threshold REFLECTIVITY will be allowed in the segment).
   Values: Default 2, range (0–5)
6) DROPOUT REF DIFF
   Definition: The difference in effective reflectivity of sample volumes below REFELECTIVITY that may still be included in a segment identified with REFLECTIVITY.
   Algorithmic response to change: Setting this threshold higher will allow more departure from REFLECTIVIIY when building a segment. Setting this threshold lower will allow less departure from REFLECTIVITY when building a segment.
   Values: Default 5 dB*Z*, range (0–10 dB*Z*)
7) ELEVATION MERGE
   Definition: Threshold elevation angle difference (vertical gap) for merging cells that are in close proximity.
   Algorithmic response to change: Setting this threshold lower will permit more cells, in close proximity, to maintain their identity. Setting the threshold higher will cause fewer detections of closely spaced cells. The more cells that are allowed to be declared within close proximity (i.e., the lower the threshold), the more difficult time association becomes for the tracking process.

Values: Default 3.0°, range (1.0°–5.0°)

8) HEIGHT MERGE

Definition: Threshold vertical gap distance for merging cells in close proximity.

Algorithmic response to change: Setting this threshold lower will permit more cells, in close proximity, to maintain their identity. Setting the threshold higher will cause fewer detections of closely spaced cells. The more cells that are allowed to be declared within close proximity (i.e. the lower the threshold), the more difficult time association becomes for the tracking process.

Values: Default 4.0 km, range (1.0–8.0 km)

9) HORIZONTAL DELETE

Definition: Threshold distance for deleting storms in close proximity.

Algorithmic response to change: A larger value will result in fewer detections and can cause poor tracking performance in highly evolving situations.

Values: Default 5.0 km, range (3.0–30.0 km)

10) HORIZONTAL MERGE

Definiton: Threshold horizontal distance for merging cells that are in close proximity.

Algorithmic response to change: Setting this threshold lower will permit more cells, in close proximity, to maintain their identity. Setting the threshold higher will cause fewer detections of closely spaced cells. The more cells that are allowed to be declared within close proximity (i.e., the lower the threshold), the more difficult time association becomes for the tracking process.

Values: Default, 10.0 km range (5.0–20.0 km)

11) NUMBER OF SEGMENTS

Definition: Minimum number of segments required to save a 2D component.

Algorithmic response to change: Fewer storms are detected at longer ranges when NUMBER OF SEGMENTS is set too high. False detections caused by ground clutter are virtually eliminated when the parameter is set above two. Setting the parameter to one will cause 2D storm components to be built for clutter, but these generally do not pass the vertical continuity requirement to be declared as a storm.

Values: Default 2, range (1–4)

12) REFLECTIVITY 1–7

Definition: The seven reflectivity thresholds used for the one-and two-dimensional parts of the storm cell building process (60–30 dB*Z*).

Algorithmic response to change: Phenomenon with chosen reflectivity thresholds will be detected if they meet the requirements of the storm cell building process.

Values: Default 60, 55, 50, 45, 40, 35, 30 dB*Z*, range (0–maximum detectable dB*Z* value).

13) SEGMENT LENGTH 1–7

Definition: Minimum required length of a segment.

Algorithmic response to change: Lowering this parameter will cause the detection of more smaller storms and raising this parameter will decrease the number of detections.

Values: Default 1.9 km, range (1.9–9.9 km)

14) SEGMENT OVERLAP

Definition: Minimum range overlap required for grouping segments into 2D components.

Algorithmic response to change: This parameter should never be lower than the gate spacing of the reflectivity data. The effect of lowering this parameter is unknown at this time. Raising this parameter will cause fewer detections of smaller storms and becomes meaningless without a corresponding change in the area thresholds (COMPONENT AREA).

Values: Default 2, range (0–5 bins)

15) SPEED

Definition: Speed used to compute the correlation distance.

Algorithmic response to change: Changing this value will cause storms moving slower or faster than SPEED to have less chance of correct time association.

Values: Default 30 m s^{-1}, range (10–99 m s^{-1})

16) TIME

Definition: Maximum time between successive volume scans for the storm cell histories to be retained for tracking and trending.

Algorithmic response to change: Setting this value lower will cause storms to not be correctly time associated when a gap in the data occurs that is shorter than TIME. Setting this value higher will cause storm to be time associated (not necessarily correctly) when a gap in the data occurs that is shorter than TIME.

Values: Default 20 min, range (10–60 min)

APPENDIX B

Cell-Based Vertically Integrated Liquid

The liquid water content of a cloud can be used to determine the amount of condensation and dynamic development that has taken place. Changes in the liquid water content are also associated with thermodynamic energy changes (Greene and Clark 1972). VIL, a measure of the liquid water in a vertical column within a storm, was calculated using the reflectivity data. VIL is given by

$$\mathrm{VIL} = \sum_{i=1}^{n} 3.44 \times 10^{-6} \left[\frac{(Z_i + Z_{i+1})}{2} \right]^{4/7} \Delta h \qquad (\mathrm{kg\ m^{-2}}), \tag{B1}$$

where Z_i and Z_{i+1} are reflectivity factors at two successive levels and Δh is the distance (m) between the levels (Stewart 1991). Thus, VIL increases with both the magnitude and depth of the reflectivity. Typically, VIL is

calculated within 3 × 5 km horizontal ''bins'' (Stewart 1991). However, in SCIT we calculate VIL by using a three-gate-averaged maximum reflectivity at each level and then vertically integrate through the depth of the storm. This method, hereafter known as cell-based VIL, was chosen to account for any tilt that may be present within the core of the storm. Cell-based VIL is, in no way, meant to imply that a downdraft would fall along a slanted vertical path. It is simply a measure of the liquid water content of the reflectivity core that may not be entirely captured by a grid-based VIL calculation. In addition, cell-based VIL unlike grid-based VIL, can easily be displayed along with other storm cell characteristics in alphanumeric tables and trend plots.

REFERENCES

Boak, T. I. S., III, A. J. Jagodnik Jr., R. B. Marshall, D. Riceman, and M. J. Young, 1977: Tracking and significance estimator. R&D Equipment Information Rep., Contract AFGL-TR-77-0259, Raytheon, Wayland, MA, 118 pp. [Available from Raytheon Company, 141 Spring St., Lexington, MA 02173.]

Brady, P. J., M. J. Schroeder, and M. R. Poellot, 1978: Automatic identification and tracking of radar echoes in HIPLEX. Preprints, *18th Conf. on Radar Meteorology*, Atlanta, GA, Amer. Meteor. Soc., 139–143.

Burgess, D. W., R. Lee, S. Parker, L. Floyd, and D. L. Andra, 1995: A study of minisupercells observed by WSR-88D radars. Preprints, *27th Int. Conf. on Radar Meteorology*, Vail, CO, Amer. Meteor. Soc., 4–6.

Crane, R. K., 1979: Automatic cell detection and tracking. *IEEE Trans. Geosci. Electron.*, **GE-17,** 250–262.

Crum, T. D., and R. L. Alberty, 1993: The WSR-88D and the WSR-88D Operational Support Facility. *Bull. Amer. Meteor. Soc.*, **74,** 1669–1687.

Davies, J. M., and R. H. Johns, 1993: Some wind and instability parameters associated with strong and violent tornadoes, 1, Wind shear and helicity. *The Tornado: Its Structure, Dynamics, Prediction, and Hazards, Geophys. Monogr.*, No. 79, Amer. Geophys. Union, 573–582.

Dixon, M., and G. Wiener, 1993: TITAN: Thunderstorm identification, tracking, analysis and nowcasting—A radar-based methodology. *J. Atmos. Oceanic Technol.*, **10,** 785–797.

Forsyth, D. E., 1979: Real time forecasting of echo–centroid motion. M.S. thesis, Dept. of Meteorology, University of Oklahoma, 79 pp. [Available from University of Oklahoma, Norman, OK 73019.]

Greene, D. R., and R. A. Clark, 1972: Vertically integrated liquid: A new analysis tool. *Mon. Wea. Rev.*, **100,** 548–552.

Jackson, M. E., 1993: An echo motion algorithm for air traffic management using a national radar mosaic. Preprints, *Fifth Int. Conf. on Aviation Weather Systems*, Vienna, VA, Amer. Meteor. Soc., 299–303.

——, and R. T. Jesuroga, 1995: The ATMS convective area guidance product. Preprints, *Sixth Conf. on Aviation Weather Systems*, Dallas, TX, Amer. Meteor. Soc., 78–82.

Klazura, G. E., and D. A. Imy, 1993: A description of the initial set of analysis products available from the NEXRAD WSR-88D system. *Bull. Amer. Meteor. Soc.*, **74,** 1293–1311.

Klingle-Wilson, D., E. Mann, and A. Denneno, 1993: The Integrated Terminal Weather System (ITWS) Storm Cell Information and Weather Impacted Airspace Detection Algorithm. Preprints, *Fifth Int. Conf. on Aviation Weather Systems*, Vienna, VA, Amer. Meteor. Soc., 40–44.

NSSL, cited 1995: Fort Worth–WDSS Proof-of-Concept test follow-up survey results. [Available online from http://www.nssl.noaa.gov/srad/swat/ftw.survey.html.]

Rosenfeld, D., 1987: Objective method for analysis and tracking of convective cells as seen by radar. *J. Atmos. Oceanic Technol.*, **4,** 422–434.

Sanger, S. S., R. M. Steadham, J. M. Jarboe, R. E. Schlegel, and A. Sellakannu, 1995: Human factors contributions to the evolution of an interactive Doppler radar and weather detection algorithm display system. Preprints, *11th Int. Conf. on Interactive Information and Processing Systems for Meteorology, Oceanography, and Hydrology*, Dallas, TX, Amer. Meteor. Soc., 1–6.

Stewart, S. R., 1991: The prediction of pulse-type thunderstorm gusts using vertically integrated liquid water content (VIL) and the cloud top penetrative downdraft mechanism. NOAA Tech. Memo. NWR SR-136, 20 pp. [Available from National Technical Information Service, U.S. Dept. of Commerce, 5285 Port Royal Rd., Springfield, VA 22161.]

Stumpf, G. J., A. Witt, E. D. Mitchell, P. L. Spencer, J. T. Johnson, M. D. Eilts, K. W. Thomas, and D. W. Burgess, 1998: The National Severe Storms Laboratory Mesocyclone Detection Algorithm for the WSR-88D. *Wea. Forecasting*, **13,** 304–326.

Wilk, K. E., and K. C. Gray, 1970: Processing and analysis techniques used with the NSSL weather radar system. Preprints, *14th Radar Meteorology Conf.*, Tucson, AZ, Amer. Meteor. Soc., 369–374.

Wilks, D. S., 1995: *Statistical Methods in the Atmospheric Sciences*. Academic Press, 467 pp.

Zittel, W. D., 1976: Computer applications and techniques for storm tracking and warning. Preprints, *17th Conf. on Radar Meteorology*, Seattle, WA, Amer. Meteor. Soc., 514–521.